BOZORTH, R. M. (1923). *J. Amer. Chem. Soc.* **45**, 1621.
BUERGER, M. J. (1935). *Amer. Min.* **20**, 36.
BURBANK, R. D. (1951). *Acta Cryst.* **4**, 143.
COCHRAN, W. (1948). *Acta Cryst.* **1**, 138.
FRUEH, A. J. (1951). *Amer. Min.* **36**, 833.
GILLIS, J. (1948). *Acta Cryst.* **1**, 174.
HARKER, D. (1948). *Amer. Min.* **33**, 764.
HARKER, D. & KASPER, J. S. (1948). *Acta Cryst.* **1**, 70.
ITO, T. (1937). *Beitr. Min. Japan.* N.F. **2**, 6.
ITO, T. (1950). *X-ray Studies on Polymorphism.* Tokyo: Maruzen.
LU, C. S. & DONOHUE, J. (1944). *J. Amer. Chem. Soc.* **66**, 818.
PAULING, L. (1940). *The Nature of the Chemical Bond.* Ithaca: Cornell University Press.

Acta Cryst. (1952). **5**, 782

The Interpretation of Electron-Diffraction Patterns from One-Degree-Orientated Polycrystalline Deposits and Rotated Crystals

BY H. WILMAN

Applied Physical Chemistry Laboratories, Imperial College, London S.W. 7, England

(*Received* 8 *April* 1952)

Effective practical methods are developed for interpreting electron-diffraction patterns from one-degree-orientated polycrystalline deposits or rotating crystals, to determine their orientation, and their lattice form where this is not known previously. These methods apply to crystals of any symmetry; all apply to the case where the orientation axis is normal to the electron beam or nearly so, while some are of quite general application.

1. Introduction and general basis

Thin polycrystalline films of many materials are now much used in research and industry, and their properties depend much on structural characteristics such as crystal size, orientation, habit and purity. Many electron-diffraction investigations have shown that in such deposits formed under certain conditions on epitaxially inert substrates the crystals tend to grow in a 'one-degree' orientation, i.e. with a certain type of lattice row $[UVW]$ in common but otherwise with random disposition about this common axis. The deposit then yields an electron-diffraction pattern approximating to that which would be obtained by rotating a single crystal round the $[UVW]$ lattice row placed parallel to the orientation axis. The interpretation of such patterns obtained with fast electrons is now discussed, and an experimental study (Evans & Wilman, 1952) has also led to a clearer understanding of the causes and nature of preferred orientation in deposits condensed from the vapour.

The method of interpretation of such patterns first proposed by Kirchner (1932) (cf. also Thomson, Stuart & Murison, 1933; Nelson, 1937; and Thomson & Cochrane, 1939) is unduly laborious. A simpler Laue-zone method has been described (Finch & Wilman, 1937*a*, *b*) by which the theoretical pattern expected from the crystals in any suggested one-degree orientation can be constructed more easily for comparison with the recorded pattern. The present work describes a new generalized extension of this method which makes it easily applied to all types of lattice, and further new methods which have proved useful in recent studies of orientation in deposits formed chemically (Goswami, 1950) or by condensation from the vapour (Evans, 1950; Evans & Wilman, 1952).

Single-crystal rotation patterns and also often one-degree-orientation patterns have, as in X-ray diffraction work, an important application for determining the lattice form and dimensions where these are not known initially, hence methods suitable for this purpose are also developed below for the case of patterns where the diffractions lie on elliptic or hyperbolic loci (see Finch & Wilman, 1936*b*, 1937*a*, *b*; Uyeda, 1938; Goche & Wilman, 1939). In the simpler case of patterns in which well-defined 'layer lines' (and often also 'row lines') occur, the methods described for analysis of the analogous X-ray patterns by Buerger (1942), Bunn (1945) and Henry, Lipson & Wooster (1951) are readily adapted and need not be discussed further here.

In polycrystalline deposits the criterion for one-degree orientation is (in reflexion patterns) that the diffraction pattern is unchanged as the azimuth of the electron beam round the orientation axis is varied, or (in transmission) that only a ring pattern is obtained when the beam is along the orientation axis, although the rings break up into arcs and arcs also appear on other ring positions on inclining the specimen (Thomson, 1930; Finch & Quarrell, 1933*a*, *b*). In certain cases the axis of one-degree orientation can be oblique to the substrate (Burgers & Dippel, 1934; Burgers & Ploos van Amstel, 1936; Beeching, 1936; Nelson, 1937; Schulz, 1949; Evans & Wilman, 1952).

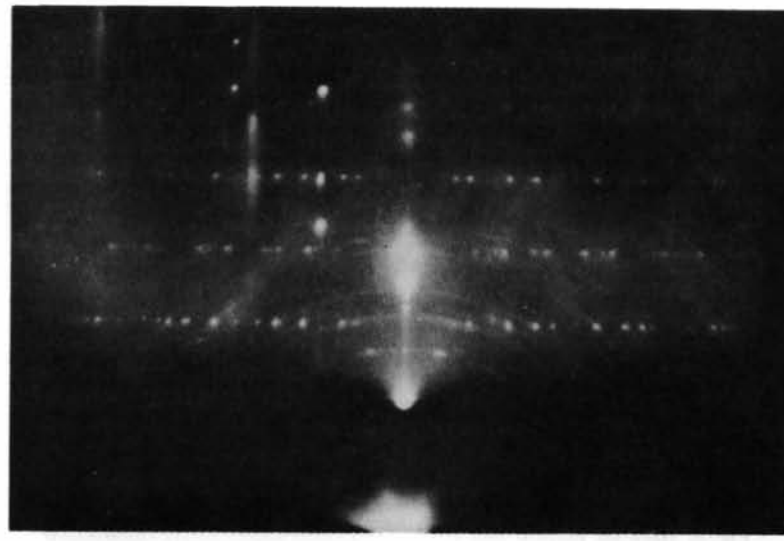

Fig. 1. Layer-line pattern from silver nitrate, showing high perfection of orientation sometimes obtained in deposits formed on substrates which are atomically highly smooth, in this case smooth {111} faces of silver crystals on a muscovite mica cleavage face.

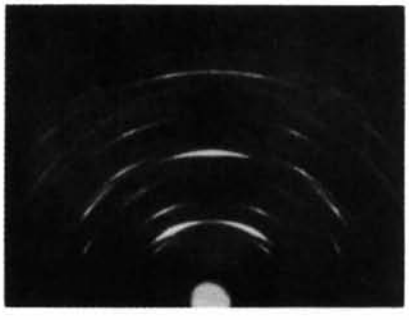

Fig. 2 (*a*). Arc pattern from $\{11\bar{2}2\}$-orientated zinc condensed on a rocksalt cleavage face.

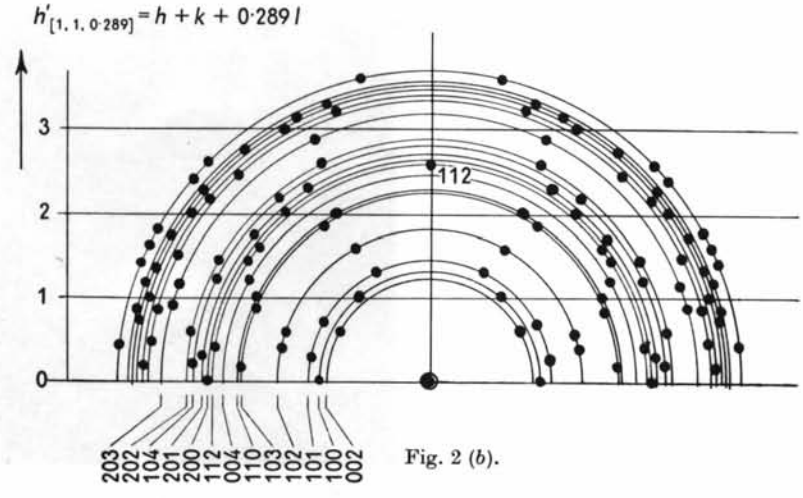

Fig. 2 (*b*).

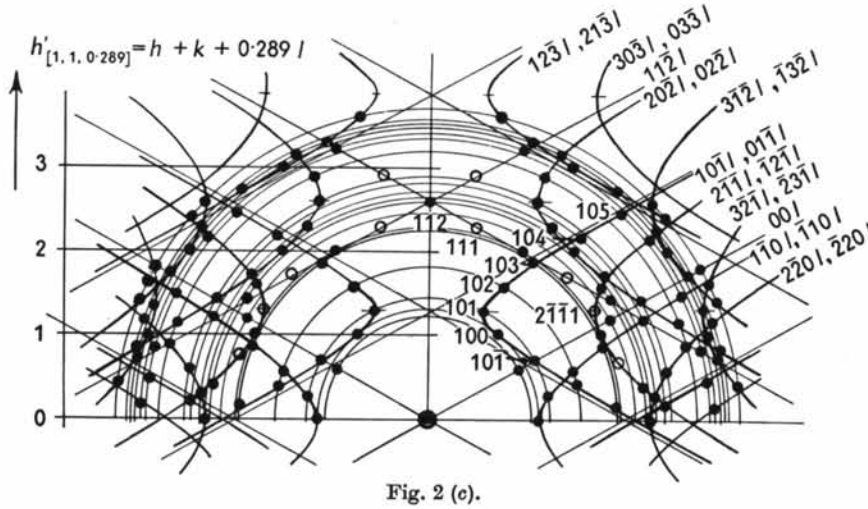

Fig. 2 (*c*).

[*To face p.* 782]

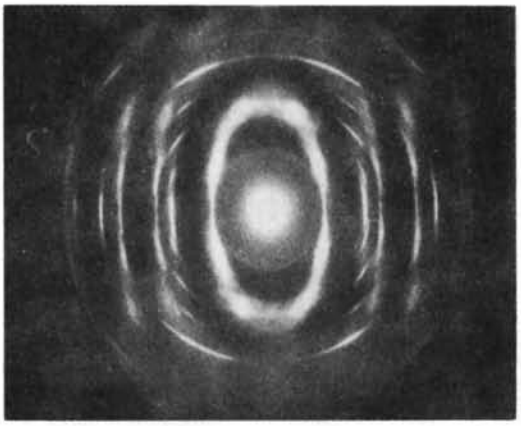

Fig. 3. Arcs on elliptic loci from (0001)-orientated CdI_2; orientation axis inclined to beam (its projection is vertical in Fig. 3).

Fig. 4. Hyperbolic loci of diffraction groups from a single MoS_2 crystal rotated about an axis normal to beam (its projection is vertical in Fig. 4).

Although the crystals often tend to grow initially on the substrate with a more or less densely-populated net plane (HKL) parallel to the substrate (cf. however the 'outward growth' type of orientation in electrodeposits, with a densely-populated lattice row normal to the substrate (Finch, Wilman & Yang, 1948)), usually there is some spread from the mean due to substrate roughness and other causes (see Evans & Wilman, 1952). The pattern then consists of arcs (Fig. 2(a)) instead of spots (Fig. 1). The HKL diffraction and its higher orders are centred on the plane of incidence and correspond to the Bragg reflexions from the plane (HKL), thus the radial distance of this diffraction from the undeflected-beam spot often gives direct identification of the indices of this plane which is normal to the orientation axis. If the arcs are unduly long, or if there is no simple diffraction on the plane of incidence, other diffraction positions have to be used to indicate the mean orientation, followed by detailed check of all the diffraction positions. The length of, and intensity distribution along, the HKL arc or its higher orders gives directly the extent and nature of the spread of orientation from the mean (HKL) orientation.

2. New methods of interpretation

2·1. *The generalized Laue-zone method of interpretation*

If the lattice translation, $\mathbf{T}$, along the orientation axis has indices $[UVW]$ and has normal to it the plane (HKL), which usually lies parallel to the substrate, the explicit expressions for U, V, W, in terms of H, K, L (hitherto apparently lacking in the literature) are simply derived as follows:

$$\mathbf{T} = U\mathbf{a}+V\mathbf{b}+W\mathbf{c} = \mathbf{r}^*_{HKL}.Td_{HKL},$$
$$\mathbf{r}^*_{HKL} = H\mathbf{a}^*+K\mathbf{b}^*+L\mathbf{c}^* = (\mathbf{r}^*_{HKL}.\mathbf{a}^*)\mathbf{a}+(\mathbf{r}^*_{HKL}.\mathbf{b}^*)\mathbf{b}+(\mathbf{r}^*_{HKL}.\mathbf{c}^*)\mathbf{c},$$

whence

$$U:V:W = \mathbf{r}^*_{HKL}.\mathbf{a}^*:\mathbf{r}^*_{HKL}.\mathbf{b}^*:\mathbf{r}^*_{HKL}.\mathbf{c}^* \quad (1)$$

$$\left.\begin{aligned} =(1/a)\{&(H/a)\sin^2\alpha+(K/b)(\cos\alpha\cos\beta-\cos\gamma)\\ &+(L/c)(\cos\gamma\cos\alpha-\cos\beta)\}:\\ (1/b)\{&(H/a)(\cos\alpha\cos\beta-\cos\gamma)+(K/b)\sin^2\beta\\ &+(L/c)(\cos\beta\cos\gamma-\cos\alpha)\}:\\ (1/c)\{&(H/a)(\cos\gamma\cos\alpha-\cos\beta)\\ &+(K/b)(\cos\beta\cos\gamma-\cos\alpha)+(L/c)\sin^2\gamma\}. \end{aligned}\right\} \quad (2)$$

Conversely, the indices (HKL) of the plane which is normal to the lattice row $[UVW]$, so that $[HKL]^*$ is normal to $(UVW)^*$, are given by

$$H:K:L=(Ua^2+Vab\cos\gamma+Wca\cos\beta):(Uab\cos\gamma+Vb^2+Wbc\cos\alpha):(Uac\cos\beta+Vbc\cos\alpha+Wc^2). \quad (3)$$

Thus, when the type of orientation plane (HKL) is more or less clearly indicated, for example by its strong Bragg reflexion arc which usually occurs in the plane of incidence of the reflexion pattern obtained at grazing incidence of the electron beam on the deposit, then the following procedure may be used to test this conclusion. First from the expression (2) convenient values U, V, W (not necessarily integers) are obtained defining the normal to (HKL); then the practically straight and equidistant Laue zones ('layer lines') of constant Laue index h' relative to the corresponding vector $\mathbf{T}_{UVW}$ can be drawn normal to the projection of $\mathbf{T}_{UVW}$ on the plate, at convenient intervals on a diagram showing the powder-pattern ring positions, as in Fig. 2(b). The h'th zone is distant $h'\lambda L/T_{UVW}\sin\psi$ from the undeflected-beam spot, to a close approximation, when the angle ψ between $\mathbf{T}_{UVW}$ and the electron beam is not small. Since, however, any diffraction which has Laue indices hkl relative to $\mathbf{a}$, $\mathbf{b}$, $\mathbf{c}$ has an index h' given by

$$h' = hU+kV+lW \quad (4)$$

relative to $\mathbf{T}_{UVW}$, the scale of h' on the diagram is most conveniently obtained from the radius R_{HKL} of the HKL ring on which the HKL diffraction lies at the point where the h'_{HKL}th zone is tangent to it, for which

$$h' = h'_{HKL} = HU+KV+LW. \quad (5)$$

Thus the distance apart of the zones per unit of h' is

$$D_1 = R_{HKL}/h'_{HKL} = R_{HKL}/(HU+KV+LW). \quad (6)$$

In this way the $\mathbf{T}_{UVW}$ zones can be drawn at $h' = 0, 1, 2, 3, \ldots$ or desired submultiples of these values, whence direct interpolation is easy, to find the point where any particular diffraction hkl lies, at the intersection of the hkl ring with the h'th zone defined by (4). On any hkl ring account must of course be taken of all the diffractions corresponding to the symmetrically equivalent planes of form $\{hkl\}$.

For the crystallographic systems of higher symmetry than triclinic the expression (2) reduces to the following simpler ones:

Monoclinic:

$$U:V:W=(1/a)\{(H/a)-(L/c)\cos\beta\}:(1/b)\{(K/b)\sin^2\beta\}:(1/c)\{-(H/a)\cos\beta+(L/c)\}.$$

Rhombohedral:

$$U:V:W=\{H(1+\cos\alpha)-(K+L)\cos\alpha\}:\{K(1+\cos\alpha)-(H+L)\cos\alpha\}:\{L(1+\cos\alpha)-(H+K)\cos\alpha\}.$$

Hexagonal:

$$U:V:W=(2H+K):(H+2K):(\tfrac{3}{2})L/(c/a)^2.$$

Orthorhombic:

$$U:V:W=H/a^2:K/b^2:L/c^2.$$

Tetragonal:

$$U:V:W=H:K:L/(c/a)^2.$$

Cubic:

$$U:V:W=H:K:L.$$

2·2. *The 'row-line' method*

An independent method, complementary to that of § 2·1, for determining the positions of the diffractions associated with any trial orientation, is to define these, near the undeflected beam, as the intersections made with the appropriate Hull–Debye–Scherrer ring positions by the loci which are similar to, but λL times larger than, the loci traced out on the Ewald 'sphere of reflexion' by a set of parallel reciprocal-lattice rows during rotation of the lattice round the orientation axis. The part of the Ewald sphere concerned, for fast electrons, is that surrounding the origin, and since it is closely approximated by the tangent plane at the origin this will be referred to below as the 'Ewald plane'.

(*a*) *General expressions defining the row-line loci.*— To construct such loci the equations previously derived can be used (Finch & Wilman, 1936*b*, 1937*a*; Goche & Wilman, 1939). In Fig. 5, O is the origin of the

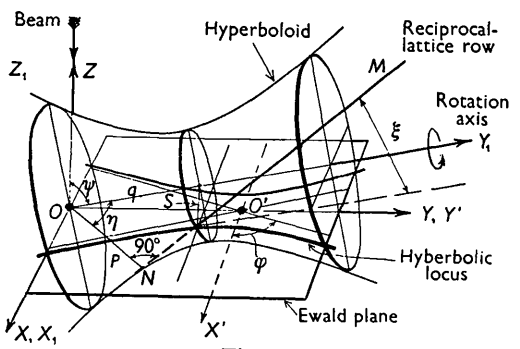

Fig. 5.

reciprocal lattice, ZO is the electron beam, $OXYZ$ are orthogonal and OY is the projection of the rotation axis OY_1 on the XY plane; $\psi = \angle\ Y_1OZ$, $\eta = \angle\ NOY_1$ ξ is the angle between the lattice row MN and OY_1, and p is the perpendicular ON from O to the row concerned. During the rotation a row MN in general generates a hyperboloid of revolution as in Fig. 5, and intersects the Ewald plane in a point which traces out a conic whose centre O' is at

$$x_c=0;\ y_c=-p\cos\eta\sin\psi/(\cos^2\psi-\sin^2\xi)\ , \quad (8)$$

the equation of the conic relative to parallel axes $O'X'$, $O'Y'$ through O' being

$$x'^2\cos^2\xi+y'^2(\cos^2\psi-\sin^2\xi) = p^2\cos^2\xi[1+\{\cos^2\eta/(\cos^2\psi-\sin^2\xi)\}]\ . \quad (9)$$

The ratio of the semi-axes A and B, parallel to OX and OY respectively, is

$$B/A = \cos\xi/(\cos^2\psi-\sin^2\xi)^{\frac{1}{2}}\ . \quad (10)$$

If $p=0$, or $A=0$, the locus is the pair of straight lines through O or O' respectively, given by

$$y' = \pm x'\cos\xi/(\sin^2\xi-\cos^2\psi)^{\frac{1}{2}}\ ; \quad (11)$$

but if $p\neq 0$ the locus is a hyperbola, parabola or ellipse according to whether $(\sin^2\xi-\cos^2\psi)$ is $>$, $=$ or <0, i.e. whether $|\xi|$ is $>$, $=$ or $<|90°-\psi|$. The asymptotes of the hyperbola are the lines

$$y'=\pm x'.\cos\xi/(\sin^2\xi-\cos^2\psi)^{\frac{1}{2}}=\pm x'\tan\varphi\ , \quad (12)$$

whence

$$\sin\varphi=\cos\xi/\sin\psi\ . \quad (13)$$

When the rotation- or orientation axis is normal to the electron beam or nearly so, as in reflexions patterns, $\psi\simeq 90°$, hence $\xi\simeq 90°-\varphi$. As ξ increases, the hyperbolae become more and more acute until, when $\xi=90°$, they reduce to the straight lines normal to OY:

$$y=p\cos\eta/\sin\psi\ , \quad (14)$$

relative to O as origin, and extending outwards on each side of OY from the points where $x=p.[1-(\cos^2\eta/\sin^2\psi)]^{\frac{1}{2}}$. The rare case of $|\xi|=|90°-\psi|$ gives a parabola; and when $\xi=0$, and hence $\eta=90°$, the locus is the ellipse

$$(x^2/p^2)+(y^2/(p^2/\cos^2\psi))=1\ . \quad (15)$$

In terms of the shortest distance s between the row and the rotation axis, and the distance q from 0 along the rotation axis to the foot of this mutual perpendicular, the centre O' of the locus is at

$$x_c=0;\ y_c=-q.\sin\psi\sin^2\xi/(\cos^2\psi-\sin^2\xi)\ , \quad (16)$$

and, relative to parallel axes OX', OY' through O', the equation is

$$x'^2+y'^2(\cos^2\psi-\sin^2\xi)/\cos^2\xi = s^2+q^2\cos^2\psi\sin^2\xi/(\cos^2\psi-\sin^2\xi)\ . \quad (17)$$

A feature of the loci, whether ellipses, hyperbolae or lines, is that the perpendicular p corresponds to ($\simeq 1/\lambda L\times$) the shortest distance (the normal in the case of ellipses and hyperbolae) from the undeflected-beam spot to the locus. Note, however, that the vertices of each hyperbolic locus do not, except when $\psi=90°$, correspond to the end-point of s on the row as this point crosses the Ewald sphere during the rotation.

Equation (17) follows from the fact that the reciprocal-lattice points along each row are regularly spaced at T^* apart; thus throughout the rotation they lie on equidistant planes normal to the rotation axis and $T^*\cos\xi$ apart, intersecting the Ewald plane in equidistant lines normal to OY_1. The corresponding lines in the pattern are thus practically equidistant when ψ is not too far from 90°, at D apart (Fig. 6), where

$$D\simeq\lambda L.T^*\cos\xi/\sin\psi\ . \quad (18)$$

Also, because the intersections of the equidistant planes with the Ewald sphere correspond to some of the Laue zones of spacing $\lambda L/T\sin\psi$ associated with the crystal-lattice row T which lies along the rotation axis, $D\simeq n\lambda L/T\sin\psi$, where n is some integer. From

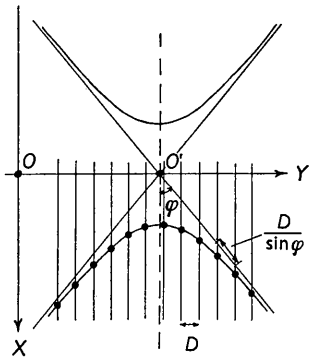

Fig. 6.

(18) and (13), or from Fig. 6, it follows that for hyperbolic loci (cf. Fig. 6), whatever ξ, we have

$$\lambda L.T^* = D/\sin\varphi\,, \qquad (19a)$$

and for elliptic loci, from (10),

$$\lambda L.T^* = D.(1-(A/B)^2)^{\frac{1}{2}}\,, \qquad (19b)$$

whence $\lambda L.T^*$ can be calculated from the measured D and φ or B/A, and thereby gives identification of the reciprocal-lattice row associated with the observed loci.

(*b*) *Elliptic loci.*—In most one-degree-orientated deposits a densely-populated net plane tends to be parallel to the substrate. Thus there is a densely-populated reciprocal-lattice row along the orientation axis, i.e. normal to the substrate. For rows in this direction $\xi = 0$ and $\eta = 90°$, and each row sweeps out a cylinder during rotation round the orientation axis. When $\psi \doteq 90°$, as in reflexion patterns, the intersection with the Ewald plane is thus a pair of straight lines parallel to OY and distant p from OY, corresponding to the 'row lines' of diffractions sometimes prominent in X-ray rotating-crystal patterns. In transmission, when $\psi \neq 90°$, the intersection is the ellipse of equation (15) with minor axis p along OX and major axis $p/\cos\psi$ along OY (Kirchner, 1932; Finch & Wilman, 1937*a*, *b*).

If the reciprocal-lattice rows parallel to the orientation axis are the most densely populated, the pattern thus consists of prominent groups of diffractions lying on these elliptic loci as in Fig. 3, all centred at the undeflected-beam spot and with axial ratio $1/\cos\psi$. (The continuous intensity distribution along ellipses for which $h+2k \neq 3n$ in Fig. 3 is due to some irregularity of stacking of the CdI_2 (0001) layers (cf. also for graphite Finch & Wilman, 1936*a*, and for clays Hendricks & Ross, 1938, and Brindley, 1951)). Fig. 7 indicates how the curvature of the Ewald sphere causes a small deviation from the above elliptic shape of the loci, with slightly unequal separation of the arcs in the symmetrical pairs near the two ends of the major axis, as seen in Fig. 3. This is also apparent from the alternative Laue-zone construction when these are defined accurately instead

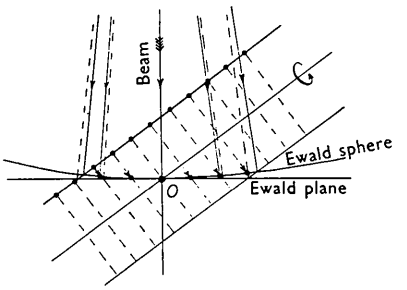

Fig. 7.

of by the approximation used in § 2·1, and it allows the direction of the orientation axis to be recognised uniquely from the pattern.

If the most densely populated reciprocal-lattice rows are not parallel to the orientation axis ($\xi \neq 0$) their intersections with the Ewald plane are circles when $\psi = 0$, as in the case of $\xi = 0$, and similarly become ellipses as ψ increases up to $90°-\xi$, but then the ellipses have different centres displaced by y_c along OY from the origin (cf. equation (8)) though their axial ratios B/A are still all equal (cf. equation (10)) and their major axes are still along OY. The variation of B/A with ψ is shown in Fig. 8 relative

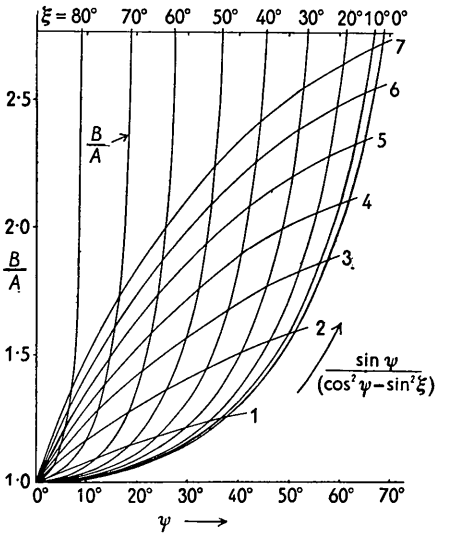

Fig. 8.

to the magnitude of ξ. Fig. 8 also indicates the magnitude of the factor $\sin\psi/(\cos^2\psi-\sin^2\xi)$ (at points on the B/A curves) in the expression (8) for y_c. These characteristics will serve for recognition of such displaced elliptic loci when they occur, and for estimation of ξ from the B/A observed at suitable inclinations ψ from the normal setting.

In the most frequent case of $\xi = 0$ the crystal translation T in the rows parallel to the orientation axis can be estimated from the spacing of the corresponding equidistant Laue zones (layer lines) on which the diffractions lie (see § 2·1 and Finch & Wilman,

1937*a*, *b*). A more accurate method is to multiply the more precisely measurable radii R of the arcs, and the semi-minor axis R_0 of the ellipse, by the factor

$$(1-\delta) = 1-\frac{3}{8}\left(\frac{R}{L}\right)^2+\frac{31}{128}\left(\frac{R}{L}\right)^4-\dots, \qquad (20)$$

to convert them to $\lambda L/d$ values, i.e. proportional to the reciprocal-lattice vectors, inversely proportional to the net-plane spacings d. A base line OP_0 is then constructed (Fig. 9) representing $R_0(1-\delta_0)$ drawn to a suitable scale, and, since this is λL times the perpendicular p from the origin to the row, at the end of it a perpendicular P_0P is erected and points $P_1, P_2, \dots$ are marked off along it, where $OP_1, OP_2, \dots$ are $R_1(1-\delta_1), R_2(1-\delta_2), \dots$ to the same scale. Fig. 9

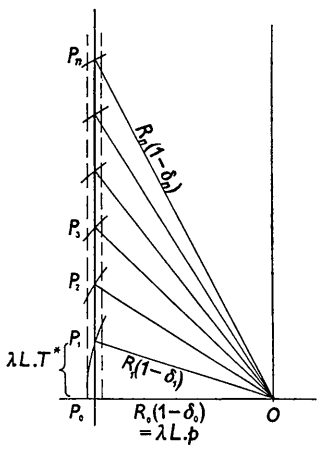

Fig. 9.

illustrates the equidistant series of points so constructed from the arcs in the second ellipse ($11l$ diffractions) in Fig. 3 from CdI_2, which is hexagonal with $a = 4{\cdot}24$ Å, $c/a = 3{\cdot}226$. This corresponds to a reciprocal-lattice row parallel to the orientation axis, and the distance apart of the points, to the scale used, is λL times the period T^*_{HKL}, i.e. λL divided by the spacing d_{HKL} of the perpendicular planes. The orientation axis can thus be identified if the lattice is known.

The minor axis of the ellipse is not accurately measurable when there is no arc at its end, and Fig. 9 shows how an inaccuracy in its estimation leads to a displacement of the successive points P which is greatest for those nearest the base line, in a manner which allows recognition of the direction of the error and location of its true position by trial. Fig. 10 shows the result when the rows are disposed so that the points do not lie on densely populated planes normal to the orientation axis, for example with (001)-orientated but monoclinic or triclinic clays. In special cases this may lead to the apparent point spacing in the diagram being a submultiple of the true spacing.

When the lattice is not previously known it can be built up from the row-line periodicity obtained as above, together with the regular lateral disposition of the rows, which is given by the lengths of the minor axes of the elliptic loci. These correspond to the p values, i.e. the radial distances from the origin to the

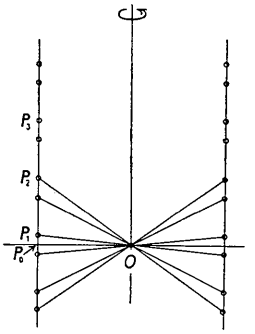

Fig. 10.

points in the two-dimensional lattice formed by the intersections of the rows with the plane normal to them through the origin. The analysis of the data to give the axial lengths and angle of this two-dimensional lattice is accomplished graphically by trial triangulations to build up this lattice from three small spacings of the group (cf. Bunn, 1945, pp. 177–8). The rows normal to this lattice and through the points of it bear reciprocal-lattice points at positions determined above (Figs. 9 and 10); thus the reciprocal lattice can be completely defined, and hence the crystal lattice.

(*c*) *Hyperbolic loci.*—When the rows not parallel to the orientation axis are the most densely-populated ($\xi \neq 0$) and when ψ is $> 90°-\xi$, i.e. $(\cos^2\psi-\sin^2\xi) < 1$, the resulting conspicuous groups of diffractions lie on the associated hyperbolic loci, as in Fig. 4 (Finch & Wilman, 1936; Uyeda, 1938; Goche & Wilman, 1939). The hyperbolae can be constructed from equation (9) for any required trial orientation for comparison with the pattern, and Fig. 11 gives the inclination of the

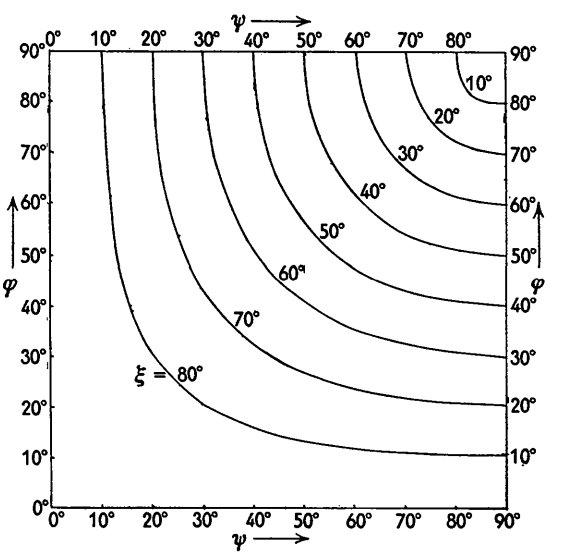

Fig. 11.

asymptotes to the real axis of the hyperbola as a function of ψ ror any given ξ value (cf. equation (13)).

Fig. 2(*c*) illustrates the application of the loci to construct the reflexion pattern expected from one-degree (11$\bar{2}$2)-orientated zinc crystals (hexagonal, $c/a = 1{\cdot}86$) using the [001]* rows which are the most densely-populated. Here $\psi \simeq 90°$, (x_c, y_c) is $(0,\ p\cos\eta/\sin^2\xi)$, the vertex is at $[\pm p\{1-(\cos^2\eta/\sin^2\xi)\}^{\frac{1}{2}},\ 0]$ and its equation relative to O' is

$$\frac{x'^2}{r^2(\sin^2\xi-\cos^2\eta)/\sin^2\xi} - \frac{y'^2}{r^2\cos^2\xi(\sin^2\xi-\cos^2\eta)/\sin^2\xi} = 1\,, \quad (21)$$

the asymptotes being the lines $y' = \pm x'\cot\xi$. The angle ξ between [112]* and [001]* is $\tan^{-1}(c/a) = 61°\,44'$. For any [001]* row through the point $[[hk0]]^*$, $r = r^*_{hk0} = 1/d_{hk0} = \{(h^2+k^2+hk).4/(3a^2)\}^{\frac{1}{2}}$, and η_{hk} is the angle between [112]* and $[hk0]^*$. Thus $\cos\eta_{hk} = \frac{1}{2}\sqrt{3}.(h+k)\{1+(a/c)^2\}^{-\frac{1}{2}}\{h^2+k^2+hk\}^{-\frac{1}{2}}$. The centre and vertex can thus be found for the loci traced out by all the [001]* rows near the origin, i.e. the $10l$, $\bar{1}0l$, $01l$, $0\bar{1}l$, $1\bar{1}l$, etc. groups of diffractions, and the loci constructed as in Fig. 2(*c*). The intersection of a particular h_1k_1 locus with the various ring positions of h_1k_1l type, where $l = 0, 1, 2, 3, \ldots$ then gives the positions of the h_1k_1l diffractions with these l values.

Hyperbolic loci of diffractions generated by a deformational curvature of parts of initially two-degree-orientated thin crystalline deposits have been described by Goche & Wilman (1939) and by Elleman & Wilman (1949), in addition to layer-line groups (for which, produced by abrasion of crystals, see Evans, Layton & Wilman, 1951).

When the crystal lattice is not already known it can be defined from the pattern as follows. The first step is to draw for each hyperbolic locus a diagram like Fig. 9 or 10, using the radial distances R from the undeflected-beam spot to the diffractions, and the distance R_0 from the undeflected spot to the nearest point of the locus. This establishes the common reciprocal-lattice period T^* along the parallel rows which correspond to the loci, and also the perpendicular distances p from the origin to the rows, together with the displacement and sequence of the lattice points from the foot of the perpendicular. The set of perpendiculars p then give, by trial as described above for the case of ellipses, the two-dimensional lattice in which the set of rows meet the plane normal to them through the origin. With the above data already obtained about the lattice-point distribution along the rows, the reciprocal lattice can thus be completely defined, and when a cell is chosen the indices of the rows corresponding to the loci can be specified, and also those of the lattice points on them.

In a transmission pattern the simplest way of determining the indices of the rotation axis is then to apply the zone-axis relations to the indices of those points on the loci which lie on a line normal to the projection of the rotation axis on the plate, i.e. parallel to the (real)axes of the hyperbolae. The reciprocal-lattice vectors to these points all lie in a plane normal to the rotation axis. It is also useful to note that ξ can be calculated from equation (13) using the experimentally known ψ and φ.

In a reflexion pattern this region lies below the shadow edge, but normally the Bragg reflexions from the plane which lies normal to the orientation axis are then more or less recognizable in the plane of incidence, and calculation of the net-plane spacing serves for its provisional identification (or use the method described in § 2·2(*a*)). Further check by the positions of the other diffractions then allows reliable determination of the orientation axis. In doubtful cases the direct calculation of the indices of the orientation axis can be attempted by the method of § 2·3. In reflexion patterns, since $\psi \simeq 90°$, $\xi \simeq 90° - \varphi$, as noted above.

2·3. *The method of calculating the orientation from the positions of three arcs, when the orientation axis is normal to the beam*

When there is one-degree orientation of not very simple type, due to various causes (see Evans & Wilman, 1952) the indices $[UVW]$ of the orientation axis, not necessarily expressed as integers in this case, or the indices (HKL) of the net plane which is normal to this axis, can in many cases be calculated in the following way, provided the orientation is strong enough to lead to patterns of short well-defined arcs. The starting point is the expression for the angle ε between the orientation axis $[UVW]$ and the reciprocal-lattice vector $\mathbf{r}^*_{hkl}$ normal to any plane (hkl):

$$\cos\varepsilon = (\mathbf{r}^*_{hkl}.\mathbf{T}_{UVW})/r^*_{hkl}T_{UVW} = (hU+kV+lW).d_{hkl}/T_{UVW}\,. \quad (23)$$

The angle ε is measurable to a close approximation in the pattern as the angle between the radii on which the (HKL) Bragg reflexion and the (hkl) reflexion lie respectively. Three such equations obtained from the observed positions and indices $h_1k_1l_1$, $h_2k_2l_2$, $h_3k_3l_3$ and the radii R_1, R_2, R_3 of three suitable arcs then give

$$U:V:W = \begin{vmatrix} k_1 & l_1 & D_1 \\ k_2 & l_2 & D_2 \\ k_3 & l_3 & D_3 \end{vmatrix} : -\begin{vmatrix} h_1 & l_1 & D_1 \\ h_2 & l_2 & D_2 \\ h_3 & l_3 & D_3 \end{vmatrix} : \begin{vmatrix} h_1 & k_1 & D_1 \\ h_2 & k_2 & D_2 \\ h_3 & k_3 & D_3 \end{vmatrix}, \quad (24)$$

where $D_n = R_n\cos\varepsilon_n (= \{\lambda L\cos\varepsilon_n\}/d_n) =$ the projection of the arc radius upon the plane of incidence.

Since in general several diffractions from symmetrically equivalent planes contribute arcs on any one ring position, one arc can be assigned definite indices $h_1k_1l_1$ from the known form for the ring on which it lies, but then all possible alternative indices must be taken into account for the other two arcs used, and finally the correct one of all the alternative solutions

must be determined by comparison (e.g. by § 2·1, 2·4 or 2·5) of the other observed arc positions with those of the corresponding constructed patterns. The indices (HKL) of the plane which is normal to the orientation axis $[UVW]$ can then be found from equation (3) if required.

Alternatively $H:K:L$ can be calculated directly. Since $\cos\varepsilon = (\mathbf{r}^*_{hkl}.\mathbf{r}^*_{HKL})/r^*_{hkl}r^*_{HKL}$,

we have
$$\begin{aligned}\cos\varepsilon/d_{hkl}d_{HKL} &= H(ha^{*2}+ka^*b^*\cos\gamma^*\\ &\quad +la^*c^*\cos\beta^*)\\ &\quad +K(ha^*b^*\cos\gamma^*+kb^{*2}+lb^*c^*\cos\alpha^*)\\ &\quad +L(ha^*c^*\cos\beta^*+kb^*c^*\cos\alpha^*+lc^{*2})\,. \qquad (25)\end{aligned}$$

Thus (25) can be expressed in the form

$$x_1H+y_1K+z_1L = (R_{HKL}/\lambda^2L^2)D_1\,, \qquad (26)$$

and, in conjunction with two further such equations corresponding to two other arcs, we obtain

$$H:K:L = \begin{vmatrix} y_1 & z_1 & D_1\\ y_2 & z_2 & D_2\\ y_3 & z_3 & D_3\end{vmatrix} : -\begin{vmatrix} x_1 & z_1 & D_1\\ x_2 & z_2 & D_2\\ x_3 & z_3 & D_3\end{vmatrix} : \begin{vmatrix} x_1 & y_1 & D_1\\ x_2 & y_2 & D_2\\ x_3 & y_3 & D_3\end{vmatrix}. \qquad (27)$$

Equation (25) reduces, for the more symmetrical systems, to a simpler expression; e.g. for the hexagonal system

$$\cos\varepsilon/d_{hkl}.d_{HKL} = (2/3a^2).[H(2h+k)+K(h+2k)+Ll\{3/(2c^2/a^2)\}]\,,$$

and thus for x_1, y_1, z_1 the proportional values $(2h+k)$, $(h+2k)$ and $3l/(2c^2/a^2)$ may be taken.

2·4. *The estimation of the orientation axis from a reflexion pattern by use of a reciprocal-lattice model*

An approximate but rapid and direct method of locating the orientation axis from a reflexion pattern which is found to be the same at all azimuths is to apply Ewald's reciprocal-lattice construction for the diffraction positions, using a three-dimensional model of the reciprocal-lattice of the material concerned, in the following way. An appropriate model is easily constructed, for example by using lengths of threaded brass rod carrying nuts at intervals to represent the lattice points and clamped parallel, in their correct positions, normal to a thin base board.

Clearly, if there is no identifiable arc in the plane of incidence of the reflexion pattern, to indicate the type of plane which is normal to the orientation axis, the arcs near the plane of incidence provide the next most direct indication of the orientation axis direction. The angle ε_1 between the radius to an $h_1k_1l_1$ arc and the plane of incidence is practically the same as the angle between the reciprocal-lattice vector $[h_1k_1l_1]^*$ and the vector $[HKL]^*$ which is along the orientation axis. The orientation axis is therefore, to a close approximation, somewhere on a cone of semi-apical angle ε_1 round the vector $[h_1k_1l_1]^*$. Similarly, if an arc of type $h_2k_2l_2$ lies on a radius at ε_2 to the plane of incidence, the axis must also lie on a cone of semi-apical angle ε_2 round one of the reciprocal-lattice rows of type $[h_2k_2l_2]^*$. It is therefore defined as one of the intersections of this cone with the first one, the correct intersection line being recognised by consideration of another arc position (or several), and finally checked by considering levels of the whole set of arcs in the pattern, using the three-dimensional model in the way indicated in § 2·5. Movement of a free rod with one end at the origin, so as to comply with the above requirements derived from the diffraction pattern, thus gives the direction of the orientation axis; its indices $[HKL]^*$ can then be estimated by inspection and a more detailed comparison pattern can be constructed, for example as in § 2·1 or 2·5.

2·5. *The method of graphical construction of the diffraction positions from a reciprocal-lattice projection*

This method of constructing the pattern corresponding to a suggested orientation is often useful

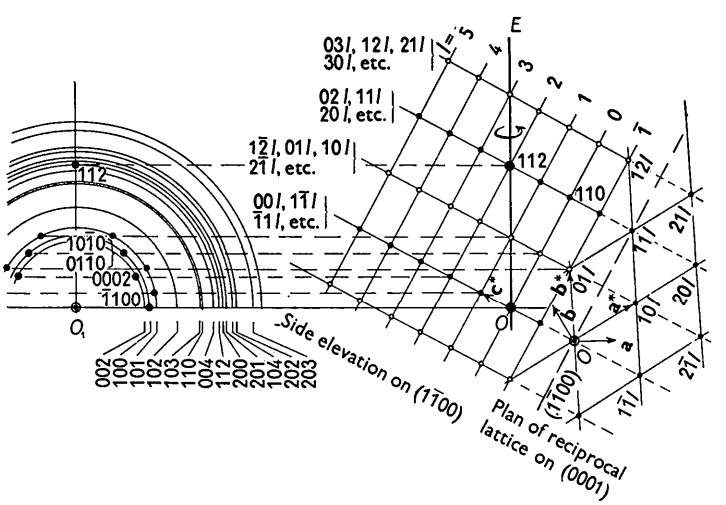

Fig. 12. Construction of diffraction positions from a reciprocal-lattice projection, exemplified for zinc in $\{11\bar{2}2\}$ orientation with orientation axis normal to the beam.

for its simplicity and its rapidity in comparing particular diffraction positions with those expected from the trial orientation. It consists primarily of constructing a projection drawing of the reciprocal-lattice upon a plane containing the orientation axis, i.e. containing the reciprocal-lattice vector $\mathbf{r}^*_{HKL}$ normal to the orientation plane (HKL). When this is done the heights of all the reciprocal-lattice points $[[hkl]]^*$ above the equator line (normal to $\mathbf{r}^*_{HKL}$) of the rotation pattern about $\mathbf{r}^*_{HKL}$ are immediately apparent and by projection normal to $\mathbf{r}^*_{HKL}$ from each lattice point $[[hkl]]^*$, to intersect the circle of radius r^*_{hkl} round the origin O or a laterally displaced new origin O_1, the position of the corresponding hkl diffraction on the hkl ring can be marked (Fig. 12).

Relatively few reciprocal-lattice projections are required in practice to cover a large range of possible orientations; for example in any type of lattice a projection on the a^* c^* plane can be applied to construct the diffraction pattern associated with any $(h0l)$ orientation, since $\mathbf{r}^*_{h0l}$ is contained in the $\mathbf{a}^*$ $\mathbf{c}^*$ plane and can be set vertical to correspond to the $h0l$-diffraction radius vector in the plane of incidence of the reflexion pattern.

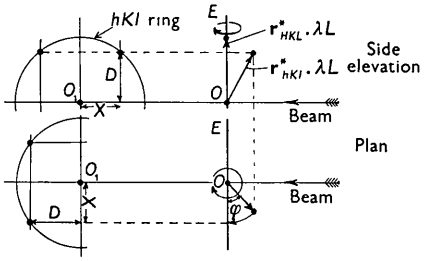

Fig. 13.

This method is also useful to estimate (Fig. 13) the azimuthal angles φ of rotation about $\mathbf{r}^*_{HKL}$, from the crystal orientation represented by the projection, to bring any particular point $[[hkl]]^*$ into the Ewald plane, shown in section by OE in Fig. 13, the primary beam being along OO_1. This, therefore, enables azimuthal crystal orientations to be determined in two-degree-orientated (epitaxial) deposits in otherwise difficult cases.

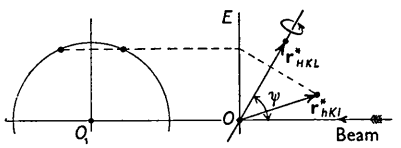

Fig. 14.

The method can also be applied (Fig. 14), like the methods of § 2·1 and § 2·2, where the orientation axis is not normal to the electron beam.

References

Beeching, R. (1936). *Phil. Mag.* (7), **22**, 938.

Brindley, G. W. (1951). *X-ray Identification and Crystal Structures of Clay Minerals.* London: Mineralogical Society.

Buerger, M. J. (1942). *X-ray Crystallography.* London: Chapman and Hall.

Bunn, C. W. (1945). *Chemical Crystallography.* Oxford: Clarendon Press.

Burgers, W. G. & Dippel, C. J. (1934). *Physica*, **1**, 549.

Burgers, W. G. & Ploos van Amstel, J. J. A. (1936). *Physica*, **3**, 1057.

Elleman, A. J. & Wilman, H. (1949). *Proc. Phys. Soc.* A, **62**, 344.

Evans, D. M. (1950). Ph.D. Thesis, London University.

Evans, D. M. & Wilman, H. (1952). *Acta Cryst.*, **5**, 731.

Evans, D. M., Layton, D. N. & Wilman, H. (1951). *Proc. Roy. Soc.* A, **205**, 17.

Finch, G. I. & Quarrell, A. G. (1933). *Nature, Lond.* **131**, 877.

Finch, G. I. & Quarrell, A. G. (1934). *Proc. Phys. Soc.* **46**, 148.

Finch, G. I. & Wilman, H. (1936*a*). *Proc. Roy. Soc.* A, **155**, 345.

Finch, G. I. & Wilman, H. (1936*b*). *Trans. Faraday Soc.* **32**, 1539.

Finch, G. I. & Wilman, H. (1937*a*). *Trans. Faraday Soc.* **33**, 1435.

Finch, G. I. & Wilman, H. (1937*b*). *Ergebn. exakt. Naturw.* **16**, 353.

Goche, O. & Wilman, H. (1939). *Proc. Phys. Soc.* **51**, 625.

Goswami, A. (1950). Ph.D. Thesis, London University.

Hendricks, S. B. & Ross, C. S. (1938). *Z. Krystallogr.* **100**, 251.

Henry, N. F. M., Lipson, H. & Wooster, W. A. (1951). *The Interpretation of X-ray Diffraction Photographs.* London: Macmillan.

Kirchner, F. (1932). *Z. Phys.* **76**, 576.

Nelson, H. R. (1938). *J. Chem. Phys.* **5**, 252.

Schulz. L. G. (1949). *J. Chem. Phys.* **17**, 1153.

Thomson, G. P. (1930). *The Wave Mechanics of Free Electrons.* New York and London: McGraw-Hill.

Thomson, G. P. & Cochrane, W. (1939). *Theory and Practice of Electron Diffraction.* London: Macmillan.

Thomson, G. P., Stuart, N. & Murison, C. A. (1933). *Proc. Phys. Soc.* **45**, 381.

Uyeda, R. (1938). *Proc. Phys.-math. Soc. Japan.* **20**, 656.